# Disruption of gastric mucous granule exocytosis by *Helicobacter pylori* virulence factor CagA

**Ryo Ninomiya**
Oita University
**Shuichi Kubo**
Oita University
**Tooru Kajiwara**
Oita University
**Hiroko Koizumi**
Oita University
**Akinori Tokunaga**
University of Fukui
**Tomohisa Uchida**
Oita University
**Hiroaki Nabeka**
Ehime University Graduate School of Medicine https://orcid.org/0000-0002-6729-8193
**Takuya Doihara**
Ehime University
**Cheng Li**
Ehime University
**Tetsuya Shimokawa**
Ehime University
**Seiji Matsuda**
Ehime University
**Naoto Kobayashi**
Ehime University
**Kazunari Murakami**
Oita University
**Toshiro Aigaki**
Tokyo Metropolitan University
**Mitsunori Fukuda**
Tohoku University, Graduate School of Life Sciences https://orcid.org/0000-0002-8620-5853
**Yoshio yamaoka**
Oita University
**Fumihiko Hamada** ( hamadaf1@oita-u.ac.jp )
Faculty of Medicine, Oita University https://orcid.org/0000-0002-9273-6036

**Article**

**Keywords:** Helicobacter pylori, gastric mucous granule exocytosis, CagA (cytotoxin-associated gene A)

**Posted Date:** January 16th, 2021

**DOI:** https://doi.org/10.21203/rs.3.rs-139758/v1

## Abstract

*Helicobacter pylori* infection is the strongest known risk factor of stomach cancer. Strains harboring the virulence factor CagA (cytotoxin-associated gene A) significantly stimulate host inflammatory response, which increases the risk of ulceration and cancer. However, the mechanisms by which CagA triggers prolonged inflammation with mucosal damage remain elusive. Based on a large-scale genetic screen using *Drosophila*, we identified a novel CagA target Synaptotagmin-like protein 2-a, Slp2-a, an effector of small GTPase Rab27. Using gastric organoid-derived monolayers of polarized mucous cells, we demonstrated that CagA inhibited Slp2-a-mediated docking of mucous granules to the plasma membrane by direct binding to Slp2-a. We further observed aberrant cytoplasmic retention of mucus in human gastric mucosa infected with CagA-expressing strains. These results suggest that CagA could be disrupting the protective mucous barrier by inhibiting Slp2-a-mediated mucous granule exocytosis, which may lead to mucosal damage from luminal acid and pepsin to promote inflammation leading to cancer.

## Introduction

*Helicobacter pylori* (*H. pylori*) is a Gram-negative bacterium infecting approximately half of humankind and has been classified as carcinogenic to humans by the World Health Organization since 1994. *H. pylori* infection has been recognized as the strongest risk factor of gastric cancer, the third leading cause of cancer-related deaths in the world[1, 2].

Infection with *H. pylori* causes life-long chronic gastric inflammation and mucosal injury that leads to atrophy, metaplasia and cancer, hence *H. pylori*-associated gastric cancer is widely recognized as an inflammation-induced cancer[2, 3]. *H. pylori* directly injects one of its virulence factors, CagA, into gastric epithelial cells using the type IV secretion system, and strongly stimulates host inflammatory response and mucosal injury, which increases the risk of gastric cancer[4–6]. It has been reported that the risk of gastric cancer by CagA-positive *H. pylori* infection is at least 5-fold higher than that of CagA-negative *H. pylori* infection[7]. As shown in Supplementary Fig. 1, CagA possesses the EPIYA (Glu-Pro-Ile-Tyr-Ala)-repeat region including a variable number of the EPIYA segments that can be classified into four types, EPIYA-A, -B, -C and -D, according to amino acid sequence variations surrounding the EPIYA tyrosine phosphorylation motif. There are several types of CagA derived from *H. pylori* found in Western countries (Western CagA), all containing EPIYA-A, EPIYA-B and different numbers of EPIYA-C (CagA ABC, CagA ABCC, CagA ABCCC), while CagA from *H. pylori* in East Asian countries has EPIYA-A, EPIYA-B and EPIYA-D (East Asian CagA or CagA ABD) which exhibits stronger carcinogenic activity than Western CagA[5, 6].

Previous cell-based biochemical studies have shown that CagA interacts with multiple host proteins, such as SHP-2[8], Grb2[9], Crk[10], Par1/MARK[11], ASPP2[12] and ZO-1[13], and directly dysregulates host cell signaling pathways and epithelial structure. However, their clinical significance is not well understood and mechanisms through which CagA triggers prolonged inflammation and progressive mucosal damage still remain elusive[3]. For example, interleukin-8 (IL-8), a chemoattractant for neutrophils, is thought to play a major role in the *H. pylori*-associated inflammatory reaction and the level of IL-8 expression has been reported to depend on CagA in gastric cancer cell lines[14–16]. However, a recent report using a human gastric epithelial organoid monolayer (gastroid monolayer) model of *H. pylori* infection demonstrated that IL-8 production showed no significant change by infection with either CagA-positive or CagA-negative *H. pylori*[17].

We demonstrate here that CagA disrupts gastric mucous granule exocytosis by inhibiting Synaptotagmin-like protein 2-a (Slp2-a), an effector of small GTPase Rab27, which functions in secretion of Rab27-bearing vesicles[18]. Our findings suggest that CagA may be promoting mucous barrier dysfunction and subsequent mucosal injury, which could stimulate host inflammatory response to promote tumorigenesis.

## Results

### CagA-induced rough eye phenotype is suppressed by co-expression of bitesize (btsz) in Drosophila.

To identify novel CagA targets, we used a GAL4/UAS ectopic expression system in *Drosophila*. In this system the yeast transcriptional activator GAL4 induces expression of transgenes containing GAL4-binding sequence UAS within their promoter[19]. When CagA was ectopically expressed under the control of eye-specific GAL4, GMR-GAL4, morphogenesis of epithelial tissues was disrupted, leading to the rough eye phenotype (*GMR-Gal4*/+; *UAS-CagA*/+ in Fig. 1a)[20]. To discover dominant modifiers of CagA-induced rough eye phenotype, we performed a genetic screen using approximately 6,000 gene search (GS) lines, in each of which a *P{GS}* vector containing UAS promoters was randomly inserted into the genome and the downstream gene was expressed in a GAL4-dependent manner[21]. We found that the eye-specific overexpression of *bitesize (btsz)*, which encodes a carboxy-terminal region containing tandem C2 domains (C2AC2B) of the Bitesize protein, strongly suppressed the CagA-induced rough eye phenotype (*GMR-Gal4/+; UAS-CagA/P{GS}17878*) (Fig. 1)[22]. These results suggest that CagA may inactivate functions of endogenous *btsz* to induce eye defects, and that mammalian homologues of *btsz* may be a novel target of CagA.

### CagA physically interacts with Synaptotagmin-like protein 2-a (Slp2-a).

The mammalian homologues of *Drosophila btsz* gene encode a synaptotagmin-like protein (Slp), of which there are five members of the family (Slp1-5)[18]. They are known to work as effectors of small GTPase Rab27 by specifically interacting with the GTP-bound form of Rab27 through their amino-terminal Slp homology domain (SHD) and function in membrane trafficking and secretion of Rab27-bearing vesicles. The carboxy-terminal region containing tandem C2 domains (C2AC2B) of Slp directly bind to phospholipids, such as phosphatidylserine (PS) and phosphatidylinositol 4, 5-bisphosphate, to promote docking of the vesicles to the inner leaflet of the plasma membrane[18, 23, 24]. Firstly, we examined the physical interaction of CagA with Slp1-5 by co-immunoprecipitation analysis and found that V5-tagged CagA ABCCC associated with T7-tagged Slp1 and Slp2-a (Fig. 2a). We decided to focus on Slp2-a, since it is predominantly expressed in the gastric surface mucous cells which provide the primary niche for *H. pylori*, and Slp2-a mutant mice show a deficiency in gastric mucus

secretion[24, 25]. Secondly, we found that C2AC2B was required and sufficient for the interaction with CagA (Fig. 2, b and c). Thirdly, we generated a series of deletion mutants of CagA lacking the EPIYA-repeat region (EPIYA), carboxy-terminal region (C-ter) and CagA-multimerization sequence (CM) within the EPIYA-repeat region (ΔEPIYA, ΔC-ter and ΔCM, respectively) and found that ΔEPIYA and ΔCM did not bind to Slp2-a (Fig. 2d and Supplementary Figs. 1 and 2)[5]. Since ΔCM may disrupt the overall structure of EPIYA (Supplementary Fig. 2), we next examined the interaction between Slp2-a and CagA ABD, which possesses a single CM in EPIYA, and confirmed that deletion of CM also abolished their interaction (ΔCM, Fig. 2, e and f)[5]. We further found that Leucine 971 (L971) in CM was an indispensable residue for the binding (L971G, substitution of Glycine for L971, Fig. 2e and Supplementary Fig. 3). These results indicate that CagA interacts with Slp2-a C2AC2B via its CM and L971 in CM is critical for the interaction (Fig. 2, c and f).

**CagA inhibits interaction between Slp2-a and phospholipids in the inner leaflet of the plasma membrane.**

The above results prompted us to investigate whether CagA inhibits the interaction between Slp2-a C2AC2B and membrane phospholipids. We first confirmed a direct interaction of recombinant hexa-histidine-tagged T7-Slp2-a C2AC2B (His-T7-Slp2-a C2AC2B) with PS immobilized on a nitrocellulose membrane (Fig. 2, g and h, and Supplementary Fig. 4)[26]. We found that the interaction was strongly inhibited by preincubation of His-T7-Slp2-a C2AC2B with a recombinant wild type CagA ABD fused with glutathione-S-transferase (GST-CagA WT), whereas preincubation with GST, GST-CagA ΔCM, or GST-CagA L971G barely affected the interaction (Fig. 2, g and h). These results suggest that CagA inhibits interaction between Slp2-a C2AC2B and phospholipids, which in turn may block the Slp-2-a-mediated docking of mucous granules to the plasma membrane.

**CagA inhibits Slp2-a-mediated docking of mucous granules to the apical plasma membrane and disrupts exocytosis in the gastric surface mucous cells.**

To examine the effects of CagA on gastric mucous granule exocytosis, we generated mouse gastric organoids predominantly composed of polarized surface mucous cells in which secretory granules containing a gel-forming mucin, MUC5AC, accumulate beneath the apical plasma membrane (Supplementary Fig. 5)[24, 27, 28]. The organoids carrying tetracycline-regulated V5-CagA ABD expression constructs were selected and its expression was induced with doxycycline (Dox) (Supplementary Fig. 6). We observed excessive mucus accumulation beneath the apical plasma membrane (arrowheads) in the CagA WT-expressing cells (Fig. 3b), whereas CagA ΔCM- and CagA L971G-expressing cells appeared the same as the control Dox (-) cells (Fig. 3, a, c and d). Ultrastructural analysis of the CagA WT-expressing cells revealed that mucous secretory granules highly accumulated beneath the apical plasma membrane (an arrow in Fig. 3f) (49.3 ± 6.5 vs 23.5 ± 5.2 in CagA WT-expressing and control cells, respectively, % of cytoplasmic area occupied by granules, Fig. 3j) (n = 5 cells in 5 organoids) and average granule size was larger than in the control cells (0.30 ± 0.015 $\mu m^2$ vs 0.13 ± 0.022 $\mu m^2$, average granule size, Fig. 3l) (Dox [+], 560 granules in 5 cells; Dox [-], 907 granules in 5 cells). Furthermore, higher magnification view of the apical surface of CagA WT-expressing cells showed that docking of granules to the apical plasma membrane was significantly inhibited (arrows in Fig. 3f') (20.9 ± 8.5 vs 55.2 ± 15.1 in CagA WT-expressing and control cells, respectively, % of docked granules per total granules < 100 nm from apical plasma membrane, Fig. 3k) (Dox [+], 196 granules in 10 cells from 10 organoids; Dox [-], 261 granules in 10 cells from 10 organoids). In contrast, CagA ΔCM- and CagA L971G-expressing cells did not show marked accumulation, increased size or docking deficit of the granules (Fig. 3, j, k and l). These results demonstrate that CagA inhibits mucous granule exocytosis by impeding docking of the granules to the apical plasma membrane.

To further clarify the role of Slp2-a in the granule-docking defect by CagA, we next examined whether exogenously expressed C2AC2B domain of Slp2-a, or GFP as a control, could reduce the interaction between CagA and granule-associated endogenous Slp2-a to restore the defect in granule docking (Supplementary Fig. 7). In the cells co-expressing CagA WT and Slp2-a C2AC2B, excessive mucus accumulation disappeared (45.0 ± 4.0 vs 15.8 ± 7.1 in CagA WT + GFP and CagA WT + Slp2-a C2AC2B, respectively, % of cytoplasmic area occupied by granules, Fig. 3, q, r and s) (n = 5 cells in 5 organoids) and reenabled granule docking (arrows in Fig. 3q' and arrowheads in Fig. 3, p' and r') (44.4 ± 9.0 vs 77.9 ± 8.1 in CagA WT + GFP and CagA WT + Slp2-a C2AC2B, respectively, % of the docked granules per total granules < 100 nm from apical plasma membrane, Fig. 3t) (Dox [+] CagA WT + GFP, 132 granules in 5 cells from 5 organoids; Dox [+] CagA WT + Slp2-a C2AC2B, 100 granules in 5 cells from 5 organoids). These results indicate that exogenous Slp2-a C2AC2B binds and traps CagA, which liberates endogenous Slp2-a from CagA and eventually allows Slp2-a-associated mucous granules to dock to the apical plasma membrane. CagA therefore inhibits docking of mucous granules to the plasma membrane and disrupts their exocytosis by a direct binding to Slp2-a.

**Excessive mucus retention in the gastric surface mucous cells of CagA-positive H. pylori-infected patients.**

Finally, we investigated whether mucus retention in the surface mucous cells could be detected in gastric biopsy specimens taken endoscopically from *H. pylori*-infected patients (14 cases of CagA-positive *H. pylori*-infected and 12 cases of CagA-negative *H. pylori* infected)[29, 30]. To observe mucus retention, gastric biopsy specimens which do not show marked atrophy (atrophy score 3) or intestinal metaplasia (intestinal metaplasia score equal to or greater than 1) were selected (see Supplementary Table 1 for further information on histological evaluation according to the updated Sydney system)[31]. As shown in Fig. 4 and Supplementary Table 1, surface mucous cells in the majority of CagA-positive *H. pylori*-infected patients had excessive mucus accumulation (13 in 14 cases), while mucus was observed only in the apical surface of those cells from CagA-negative *H. pylori*-infected patients (12 in 12 cases). This observation is consistent with our findings obtained by using gastric organoids shown in Fig. 3. These results suggest that CagA disrupts the mucous barrier by inhibiting Slp2-a-mediated mucous granule exocytosis, which may promote mucosal damage and inflammation.

## Discussion

More than twenty binding partners of CagA have been identified in cell-based biochemical studies[5, 6], however, *in vivo* significance of the interaction still remains elusive[3]. In this study, we tried an alternative *in vivo* approach in which we carried out a large-scale genetic screen using a transgenic *Drosophila* model expressing CagA in the eyes[20], and discovered a novel CagA target Slp2-a. We demonstrated that CagA disrupted mucous granule exocytosis by inhibiting functions of Slp2-a, using gastric organoid-derived monolayers of polarized mucous cells, an *in vitro* model that mimics gastric mucosa *in vivo*[32]. We further confirmed excessive mucus retention in gastric biopsy specimens from CagA-positive *H. pylori*-infected patients.

Prolonged tissue injury-induced inflammation is widely accepted as a hallmark that promotes cancer development and progression[33, 34]. Cell death leads to the release of damage-associated molecular patterns (DAMPs), such as HMGB1 (high-mobility group box-1) and ATP (adenosine triphosphate), and activates immune cells to secrete inflammatory cytokines that promote survival and proliferation of neighboring cells, initiating tumorigenesis. Our finding that CagA-positive *H. pylori* disrupts mucous granule exocytosis, which may lead to barrier dysfunction and subsequent mucosal injury, provides a novel mechanism through which CagA could be promoting inflammation and increases the risk of gastric cancer.

It has been reported that CagA disrupts tight junctions and causes loss of epithelial cell polarity with reduced transepithelial electrical resistance (TEER) in some cells, such as polarized MDCK (Madin-Darby canine kidney) cells[11, 13]. Indeed, when we expressed CagA in gastric organoid-derived polarized surface mucous cells, we also detected mislocalization of a tight junction marker ZO-1, however the effect appeared to be much milder compared with that shown in previous reports (Supplementary Fig. 8). In consistent with our results, Uotani et al. recently demonstrated that *H. pylori*-infected polarized epithelial cells of human gastroid monolayers largely maintained their normal tight and adherens junctions and TEER, although TEER transiently declined[17]. Furthermore, mucous granule accumulation only occurred beneath the apical plasma membrane and basolateral mis-sorting was not observed in the CagA-expressing cells (Figs. 3, 4, and Supplementary Fig. 9), suggesting that their cell polarity remained mostly intact. We speculate that some compensatory mechanisms may exist in the cells we used and the defect in granule docking in the CagA-expressing cells was caused by the specific inhibition of the Slp2-a C2AC2B function rather than by disruption of cellular polarity.

Finally, our finding that the exogenously expressed C2AC2B domain of Slp2-a restores the defect in mucous granule exocytosis shown in Fig. 3 is of great interest. Targeting protein-protein interactions with small molecules has been thought to be difficult, since proteins generally interact with their partner proteins using relatively large and flat contact surfaces. However, recent progress in structure-based drug design and screening technology has allowed us to make protein-protein interactions potential therapeutic targets[35, 36]. Given that the increasing rate of antibiotic resistance in *H. pylori* is a clinical challenge in the treatment of the infection in many countries[37, 38], small molecules inhibiting the interaction between CagA and Slp2-a may have potential as a novel drug candidate against mucosal damage and inflammation caused by CagA-positive *H. pylori* infection.

## Methods

### Fly genetics.

A *Drosophila* UAS-CagA (ABCC-type Western CagA derived from *H. pylori* strain G27) line was kindly provided by Prof Karen Guillemin, University of Oregon, USA[20]. A collection of approximately 6,000 GS lines generated by the Drosophila Gene Search Project (Tokyo Metropolitan University, Tokyo, Japan)[21] were obtained from the Kyoto Stock Center (Kyoto, Japan). To express transgenes in the eye, we used an eye-specific GAL4 driver, GMR-GAL4 obtained from the Bloomington Drosophila Stock Center (Indiana University, Bloomington, IN, USA). Female virgins homozygous for GMR-GAL4 and UAS-CagA (*GMR-Gal4; UAS-CagA)* were crossed with *yw* males as a wild type control or GS males which carry a *P{GS}* vector on the second or third chromosome. The eye phenotypes of the F1 progeny, *GMR-Gal4/P{GS}; UAS-CagA/+* and *GMR-Gal4/+; UAS-CagA/P{GS}* were compared with that of a control, *GMR-Gal4/+; UAS-CagA/+* using an Olympus SZX7 stereomicroscope. Culture and crosses were done at 25°C. Detailed information on the GS lines, such as insertion points of the *P{GS}* vector, was obtained from the Kyoto Stock Center website (http://kyotofly.kit.jp/stocks/documents/GS_lines.html).

### Scanning electron microscopy (SEM).

The surfaces of fly eyes were observed under a Hitachi S-4800 scanning electron microscope.

### Total RNA Isolation and real-time quantitative RT-PCR.

Total RNA from 50 adult *Drosophila* heads from a *GMR-Gal4/+; +/P{GS}17878* line or an *yw* line as a wild type control was purified with NucleoSpin RNA (Macherey-Nagel, Düren, Germany). cDNA was synthesized using a Cloned AMV First-Strand cDNA Synthesis Kit (Invitrogen, Carlsbad, CA, USA). PCR was performed on a LightCycler 96 system (Roche, Mannheim, Germany) using LightCycler FastStart DNA Master SYBR Green I reaction mix (Roche) according to manufacturer's instructions. The *btsz* primers were designed to amplify the common coding sequences in the two *btsz* transcripts, *btsz-2* (*isoform C*) and *btsz-3* (*isoform D*) (Fig. 1c). The *rpL32* gene was chosen as an endogenous control and its mRNA quantification was used for normalization. Experiments were performed in triplicate. The primers used for quantitative RT-PCR were as follows.

*rpL32* (forward), 5′-AGATCGTGAAGAAGCGCACCAAG-3′

*rpL32* (reverse), 5′-CACCAGGAACTTCTTGAATCCGG-3′

*btsz* (forward), 5′-GACACAAAGACCCGACCAGT-3′

*btsz* (reverse), 5′-CGTCCTCTACGCTGAGTTCC-3′

### Plasmids and Mutagenesis.

Expression plasmids encoding T7-tagged Slp1, 2-a, 3-a, 4-a and 5 (pEF-T7-Slp1 ~ 5) were generated as described previously[39, 40]. The Slp2-a fragments, Slp2-a SHD (amino acids 1–87) and C2AC2B (amino acids 641–950) were generated by PCR using the following primers and cloned into the pEF-T7 vector with *Bam*H I and *Sal* I sites. The resultant plasmids were designated pEF-T7-Slp2-a SHD and pEF-T7-Slp2-a C2AC2B.

SHD (forward), 5′-ACTGGATCCATGATCGACTTAAGTTTCCTG-3′

SHD (reverse), 5’- ACTGTCGACTCACTGCTCAGCTGCCGCTGG-3’

C2AC2B (forward), 5’-ACTGGATCCAACCTAGAAGTGAAAGGAAG-3’

C2AC2B (reverse), 5’-ACTGTCGACTCACTTGGAAAGCTTGGC-3’

To remove the unique *Bgl*II site (AGATCT) in the coding region of Slp2-a, a silent mutation was introduced using the KOD-Plus Mutagenesis Kit (TOYOBO, Osaka, Japan). The sequence of primers used for mutagenesis were as follows.

*Bgl*II (sense), 5’-CAGGCCTGAAGACCTGATGGAAGCCTGTG-3’

*Bgl*II (anti-sense), 5’- CACAGGCTTCCATCAGGTCTTCAGGCCTG – 3’

Using pEF-T7-Slp2-a (*Bgl*II-mutated) as a template, a Slp2-a fragment, Slp2-a ΔSHD (amino acids 82–950) was amplified by PCR using the following primers and cloned into the pEF-T7 vector with *Bam*H I and *Sal* I sites. The resultant plasmid was designated pEF-T7-Slp2-a ΔSHD.

ΔSHD (forward), 5’-ACTAGATCTCCAGCGGCAGCTGAGCAG-3’

ΔSHD (reverse), 5’-ACTGTCGACTCACTTGGAAAGCTTGGC-3’

For co-immunoprecipitation of CagA with ΔC2AC2B (amino acids 1-640) or a wild type (WT) control shown in Fig. 2c, each fragment was generated by using the following primers and cloned into a D-T7-pRc/CMV expression vector (RDB02138, provided by the RIKEN BRC through the National BioResource Project of the MEXT/AMED, Japan) with *Not* I and *Apa* I sites. The resultant plasmids were designated D-T7-pRc/CMV-Slp2-a ΔC2AC2B and D-T7-pRc/CMV-Slp2-a WT.

ΔC2AC2B (forward), 5’-ACTGCGGCCGCTATGATCGACTTAAGTTTC-3’

ΔC2AC2B (reverse), 5’-ACTGGGCCCTCAGCCAAAGTCTCCACTGTA-3’

Wild type (forward), 5’-ACTGCGGCCGCTATGATCGACTTAAGTTTC-3’

Wild type (reverse), 5’-ACTGGGCCCTCACTTGGAAAGCTTGGCAAT-3’

Plasmids encoding full-length CagA (ABCCC-type Western CagA derived from *H. pylori* strain NCTC11637) was kindly provided by Prof Masanori Hatakeyama, University of Tokyo, Tokyo, Japan[8]. The open reading frame of wild type CagA ABCCC and CagA ABCCC lacking the carboxy-terminal region, CagA ABCCC ΔC-ter (amino acids 1-1085) were amplified by PCR using following primers and cloned into an expression vector pEF6/V5-His B (Invitrogen, Carlsbad, CA, USA) with *Bam*H I and *Not* I sites. The resultant plasmids were designated pEF6/V5-CagA ABCCC and pEF6/V5-CagA ABCCC ΔC-ter.

CagA ABCCC (forward), 5’-ACTGGATCCACCATGACTAACGAAACTATTGACC-3’

CagA ABCCC (reverse), 5’-ACTGCGGCCGCCAGATTTTTGGAAACCACCTTTTG-3’

CagA ABCCC ΔC-ter (forward), 5’-ACTGGATCCACCATGACTAACGAA-3’

CagA ABCCC ΔC-ter (reverse), 5’-ACTGCGGCCGCCGCTAAAAAAACCTGCTTTAGC-3’

The CagA ABCCC lacking the EPIYA-repeat region, CagA ABCCC ΔEPIYA (amino acids 869–1086 deleted) was made by inverse PCR using the KOD-Plus Mutagenesis Kit. The resultant plasmid was designated pEF6/V5-CagA ABCCC ΔEPIYA. The sequence of primers used for mutagenesis were as follows.

CagA ABCCC ΔEPIYA-A, 5’-GATATCCGAAAAATTTTTGGCGAGA-3’

CagA ABCCC ΔEPIYA-B, 5’-CTAGAGCAAACGATAGACAAGCTCA-3’

To generate the CagA ABCCC lacking the four CagA-multimerization sequence (CM), CagA ABCCC ΔCM (amino acids 941–956, 975–990, 1009–1024, and 1043–1058 deleted), approximately 550 bases between *Nhe*I and *Xba*I sites were removed from the open reading frame of CagA ABCCC and replaced with the following double-stranded synthetic oligonucleotides CagA ABCCC ΔCM (GenScript, Tokyo, Japan) digested with *Nhe* I and *Xba* I. The resultant plasmid was designated pEF6/V5-CagA ABCCC ΔCM. The sequence of CagA ABCCC ΔCM oligonucleotides were as follows.

CagA ABCCC ΔCM (sense), 5’-
GCTAGCCCTGAAGAACCCATTTATGCTCAAGTTGCTAAAAAGGTGAATGCAAAAATTGACCGACTCAATCAAGCAGCAAGTGGTTTGGGTGGTGTAGGGCAAGCGGGCC
3’

The open reading frame of ABD-type East Asian CagA derived from *H. pylori* strain TN2 (GenBank accession No. LC007103) was amplified by PCR using following primers and cloned into an expression vector pEF6/V5-His B with *Spe* I and *Eco* RI sites. The resultant plasmid was designated pEF6/V5-CagA ABD WT (wild type).

CagA ABD (forward), 5’-CATACTAGTACCATGACTAACGAAACCATTGATC-3’

CagA ABD (reverse), 5’- ACTGAATTCGATTTCTGGAAACCACTTTTTG-3’

The CagA ABD lacking CM, CagA ABD ΔCM (amino acids 969–984 deleted) was made by inverse PCR as described above. The resultant plasmid was designated pEF6/V5-CagA ABD ΔCM. The sequence of primers used for mutagenesis were as follows.

CagA ABD ΔCM-A, 5′- GCCTGCTTGATTTGCCTCATCAAAA-3′

CagA ABD ΔCM-B, 5′- CTTTCAAGGGAACAAGAATTGACTC-3′

To perform glycine-scanning mutagenesis against conserved amino acids in CM of CagA ABD, approximately 440 bases between *Nhe*I and *Eco*47 III sites were removed from the open reading frame of CagA ABD and replaced with the following double-stranded synthetic oligonucleotides digested with *Nhe* I and *Eco*47 III. The resultant plasmids were designated pEF6/V5-CagA ABD CM- P970G, - L971G, - H974G, - D979G, - L980G, - S981G and - V983G. The sequence of oligonucleotides used for mutagenesis (GenScript) were as follows.

CagA ABD CM P970G (sense), 5′-
GCTAGCCCTGAACCCATTTACGCTACAATTGATTTTGATGAGGCAAATCAAGCAGGCTTCGGTCTTAGGAGACACGCTGCAGTTAATGATCTCAGTAAAGTAGGGCTTTC
3′

CagA ABD CM L971G (sense), 5′-
GCTAGCCCTGAACCCATTTACGCTACAATTGATTTTGATGAGGCAAATCAAGCAGGCTTCCCTGGTAGGAGACACGCTGCAGTTAATGATCTCAGTAAAGTAGGGCTTTC
3′

CagA ABD CM H974G (sense), 5′-
GCTAGCCCTGAACCCATTTACGCTACAATTGATTTTGATGAGGCAAATCAAGCAGGCTTCCCTCTTAGGAGAGGAGCTGCAGTTAATGATCTCAGTAAAGTAGGGCTTTC
3′

CagA ABD CM D979G (sense), 5′-
GCTAGCCCTGAACCCATTTACGCTACAATTGATTTTGATGAGGCAAATCAAGCAGGCTTCCCTCTTAGGAGACACGCTGCAGTTAATGGTCTCAGTAAAGTAGGGCTTTC
3′

CagA ABD CM L980G (sense), 5′-
GCTAGCCCTGAACCCATTTACGCTACAATTGATTTTGATGAGGCAAATCAAGCAGGCTTCCCTCTTAGGAGACACGCTGCAGTTAATGATGGTAGTAAAGTAGGGCTTTC
3′

CagA ABD CM S981G (sense), 5′-
GCTAGCCCTGAACCCATTTACGCTACAATTGATTTTGATGAGGCAAATCAAGCAGGCTTCCCTCTTAGGAGACACGCTGCAGTTAATGATCTCGGTAAAGTAGGGCTTTC
3′

CagA ABD CM V983G (sense), 5′-
GCTAGCCCTGAACCCATTTACGCTACAATTGATTTTGATGAGGCAAATCAAGCAGGCTTCCCTCTTAGGAGACACGCTGCAGTTAATGATCTCGGTAAAGTAGGGCTTTC
3′

To make the GST-CagA C-ter (amino acids 773–1171) proteins (Supplementary Fig. 4a), DNA fragments coding for CagA ABD C-ter WT, ΔCM and L971G (Supplementary Fig. 4a) were generated by PCR using pEF6/V5-CagA ABD WT, ΔCM and L971G as templates and cloned into pGEX-4T1 with *Eco* RI and *Xho* I sites. The sequence of used primers were as follows.

GST-CagA ABD C-ter (forward), 5′-ACTGAATTCAAGGATGTGATCATTAATCAA-3′

GST-CagA ABD C-ter (reverse), 5′-ACTCTCGAGCTATTTCTGGAAACCACTTTT-3′

To make the hexa-histidine (6 x His)-tagged T7-Slp2-a C2AC2B (amino acids 641–902) protein (Supplementary Fig. 4a), a DNA fragment coding for Slp2-a C2AC2B was amplified by PCR using following primers and cloned into pET-28b with *Bam*H I and *Eco* RI sites.

6 x His-T7-Slp2-a C2AC2B (forward),

5′-ACTGGATCCTAACCTAGAAGTGAAAGGAAG-3′

6 x His-T7-Slp2-a C2AC2B (reverse),

5′-ACTGAATTCATGTTCCAAAGCCGATCCGGA-3′

A DNA fragment containing the human ubiquitin (UbC) promoter was excised from the Piggybac transposon vector pPB-Ubc-FLIG-N[41–43] by digestion at the *Sac* II and *Bam*H I sites, and replaced with a tetracycline inducible expression cassette consisting of the TRE3GS promoter, the Transcription blocker, the human phosphoglycerate kinase 1 promoter, the Tet-On 3G transactivator gene and the SV40 poly (A) signal in the doxycycline (Dox)-inducible expression vector pTetOne (TAKARA Bio, Kusatsu, Japan). The resultant plasmid was designated pPB-TetON-FLIG-N and used for the Dox-dependent expression of GFP in gastric organoids. The sequence of PCR primers used for amplification of the tetracycline inducible expression cassette were as follows.

TetON (forward), 5′-TCCCCGCGGAGGAAGCTCGGGGCAGTG-3′

TetON (reverse), 5′-CGGGATCCTTTACGAGGGTAGGAAGTGGTACGGAAAG-3′

DNA fragments coding for V5-tagged CagA ABD- WT and - L971G were excised from pEF6/V5-His B CagA ABD WT and L971G respectively by digestion at the *Bam*H I and *Pme* I sites, and cloned into pPB-TetON-FLIG-N with *Bam*H I and *Sna*B I sites. The resultant plasmids were designated pPB-TetON-V5-CagA ABD WT and L971G. pPB-TetON-V5-CagA ABD ΔCM was made by inverse PCR using the primers CagA ABD ΔCM-A and -B as described above. The pPB-TetON-V5-CagA ABD WT, ΔCM and L971G were used for the Dox-dependent expression of V5-CagA ABDs in gastric organoids.

The Slp2-a fragment, Slp2-a C2AC2B (amino acids 638–905) was generated by PCR using the following primers and cloned into the D-T7-pRc/CMV expression vector with *Not* I and *Apa* I sites.

C2AC2B for D-T7 (forward), 5'-ACTGCGGCCGCTGACTTTGGCAACCTAGAA-3'

C2AC2B for D-T7 (reverse), 5'-ACTGGGCCCTCAGCTTTTTCCTGTTCCAAA-3'

The DNA fragment coding for D-T7-tagged Slp2-a C2AC2B (amino acids 638–902) was amplified using the following primers and cloned into pPB-TetON-FLIG-N with *Bam*H I and *Eco*R I sites. The resultant plasmid was designated pPB-TetON-T7-Slp2-a C2AC2B and used for the Dox-dependent expression of T7-Slp2-a C2AC2B in gastric organoids.

C2AC2B for pPB (forward), 5'-ACTGGATCCGCTTCCATGGCCAGCATGACC-3'

C2AC2B for pPB (reverse), 5'-ACTGAATTCATGTTCCAAAGCCGATCCGGA-3'

The pCAGGS-hyPBase was used for the expression of a hyperactive piggyBac transposase[44]. All PCR products were verified by DNA sequencing.

**Cell transfection.**

Monkey kidney fibroblast cell line COS-7 (ATCC CRL1651) was maintained in Dulbecco's modified Eagle's medium (Gibco, Grand Island, NE, USA) supplemented with 10% heat-inactivated fetal calf serum (Sigma-Aldrich, St Louis, MO, USA), 50 IU/mL penicillin and 50 μg/mL streptomycin. The COS-7 cells were seeded in 10 cm dishes at 1 x$10^5$ cells / mL and transfected with 13 μg of total DNA (10 μg for CagA and 3 μg for Slps) /dish using Lipofectamine 3000 (Invitrogen). Cells were harvested 36 hours after transfection for co-immunoprecipitation.

**Co-immunoprecipitations and Western blotting.**

Cells were pelleted and lysed in cell lysis buffer (50 mM Tris-HCl [pH 7.5], 100 mM NaCl, 5 mM EDTA, 1% Brij 35; MP Biomedicals, Santa Ana, CA, USA, Protease Inhibitor Cocktail [Roche], Phosphatase Inhibitor Cocktail; Nakalai Tesque, Kyoto, Japan). Lysates were centrifuged at 13,000 rpm at 4$^o$C for 30 min and the supernatants were incubated with protein G-Sepharose 4B (GE Healthcare Life Sciences, Little Chalfont, UK) for 1 hr at 4$^o$C. The mixture was then centrifuged for 5 sec at 13,000 rpm, and the supernatant was transferred to a fresh tube and incubated with rabbit anti-T7 antibody (MBL, Nagoya, Japan) (1:900) for 2 hrs at 4$^o$C. Protein G-Sepharose 4B was then added and incubated for 1 hr 4$^o$C. The mixture was centrifuged for 5 sec at 13,000 rpm at 4$^o$C, the supernatant was removed, and the precipitate was washed 4 times with 800 mL of cell lysis buffer. The immunoprecipitated proteins were resolved by SDS-PAGE, transferred to a polyvinylidene difluoride membrane filter (Immobilon P; Millipore, Bedford, MA, USA), and immunoblotted with antibodies described below, followed by the enhanced chemiluminescence (ECL) Prime Western blotting detection system (Amersham, Little Chalfont, UK). The following antibodies were used for immunoblotting: mouse anti-V5 monoclonal antibody (1:1,000) (R960-25; Invitrogen) and rabbit anti-T7 polyclonal antibody (1:1,000) (PM022; MBL) as primary antibodies; horseradish peroxidase (HRP)-conjugated goat anti-mouse IgG (1:2,000) (sc-2055; Santa Cruz, Dallas, TX, USA) and goat anti-rabbit IgG (1:2,000) (sc-2004; Santa Cruz) as secondary antibodies.

**Protein purification and Protein-lipid overlay assay.**

Recombinant GST-fusion proteins, GST-CagA C-ter WT, ΔCM, and L971G, were expressed in *Escherichia coli* BL21, purified by glutathione-Sepharose 4B (Amersham) and eluted from the column with elution buffer (50 mM Tris-HCl [pH 7.5], 50 mM glutathione, 200 mM NaCl). Recombinant 6 x His-T7-Slp2-a C2AC2B (His-T7-Slp2-a C2AC2B) was expressed in *Escherichia coli* BL21, purified by Ni-NTA Agarose (QIAGEN, Hilden, Germany) and eluted from the column with elution buffer (20 mM Tris-HCl [pH 8.0], 300 mM NaCl, 200 mM Imidazole). Eluted samples were resolved by SDS-PAGE and the gels were stained with Coomassie brilliant blue (Supplementary Fig. 4c). 1 μl of phosphatidylserine (1 mg/mL) (Echelon Biosciences, Salt Lake City, UT, USA) dissolved in chloroform-methanol-1N HCl (80: 80□1) was spotted onto a nitrocellulose membrane (GVS Japan, Tokyo, Japan) and air-dried. The membranes were blocked with blocking buffer (5% skim milk and 1% bovine serum albumin [BSA] in Phosphate-Buffered Saline [PBS]) for overnight at room temperature. Blots were washed 4 times with washing buffer (0.1% Tween 20 in PBS [PBS-T]) and incubated with the recombinant proteins in PBS-T (1.3 μg/mL for GST-fusion proteins and 0.03 μ g/mL for His-T7-Slp2-a C2AC2B) overnight at room temperature. After washing 4 times with PBS-T, bound His-T7-Slp2-a C2AC2B was detected using rabbit anti-T7 polyclonal antibody (1:1,000) (PM022; MBL) as a primary antibody and HRP-conjugated goat anti-rabbit IgG (1:2,000) (sc-2004; Santa Cruz) as secondary antibody followed by the ECL Western blotting detection system (Amersham). The signals were visualized using ImageQuant LAS 4000 (GE Healthcare Life Sciences) and the signal intensities were quantified using ImageQuant TL software (GE Healthcare Life Sciences).

**Isolation of fundic glands.**

All experiments using mice were approved by the Oita University Animal Ethics Committee and performed according to the Committee's guideline. The stomach extracted from BALB/c mice (6 weeks old) was opened along the greater curvature, washed with ice-cold PBS. The fundus was isolated, cut in small fragments (< 5 mm pieces) and placed into a 15 mL conical tube with ice-cold PBS. After washing with ice-cold PBS until the supernatant was clear, the fragments were treated with TrypLE Express (Gibco) at 37$^o$C for 30 min with shaking. After removal of the TrypLE Express, the fragments were suspended in dissociation buffer (1% D-solbitol and 1.5% Sucrose in PBS) and the tube was orientated perpendicular to the ground and shaken in hand for 2 min at 2 cycles

per sec. After washing with ice-cold PBS, the fragments were resuspended in 10 mL of ice-cold PBS and passed through a 70 μm Falcon cell strainer to remove cell debris and isolate fundic glands.

**Gene transfer into fundic glands, generation of fundic organoids predominantly composed of polarized surface mucous cells and induction of transgene expression.**

Isolated fundic glands (2 x$10^3$ glands) were resuspended in 100 μL of OPTI-MEM (Gibco) containing 10 μg/100 μL pPB-TetON-V5-CagA ABD WT, ΔCM or L971G, and 5 μg/100μL pCAGGS-hyPBase. For Fig. 3, m-r, 10 μg/100 μL pPB-TetON-T7-Slp2-a C2AC2B or pPB-TetON-FLIG-N was added to the solution above. Electroporation was carried out using NEPA21 (NEPA Gene, Chiba, Japan) under the condition as follows: poring pulse (pulse voltage 150 V; pulse width 5 msec; pulse number 2) and transfer pulse (pulse voltage 20 V; pulse width 50 msec; pulse number 5). After electroporation, 500 fundic glands in 50 μL of Matrigel (BD Biosciences, San Jose, CA, USA) containing growth factors, 25% L-WRN (Wnt3A, R-spondin3, Noggin) conditioned medium[45], 100 ng/mL FGF10 (PeproTech, Rocky Hill, NJ, USA), 10 nM Gastrin1 (Sigma-Aldrich), 1 mM N-acetylcysteine (Sigma-Aldrich), 50 ng/mL EGF (Sigma-Aldrich), and 10 μM Y-27632 (Sigma-Aldrich), were seeded in 24-well plates and overlaid with 500 μL of basal culture medium containing Advanced DMEM/F12 (Invitrogen) supplemented with N2 (Sigma-Aldrich), B27 (Invitrogen), GlutaMax (Invitrogen), 10 mM HEPES (Invitrogen), and Penicillin/Streptomycin (Wako, Osaka, Japan). Every 3–4 days the medium was replaced with growth factor-supplemented fresh basal culture medium containing 150 μg/mL G418 (Gibco) to select fundic organoids with the Dox-dependent expression construct and a neomycin-resistant gene derived from the pPB-TetON vector. 14 days later, the medium was replaced with fresh basal culture medium supplemented with 50 ng/mL EGF and 10 μM Y-27632 to direct fundic epithelium differentiate into surface mucous cell lineage. 3 days later, 3 μg/mL Dox (Wako) was added to the medium to induce transgene expression.

**Fixation, embedding, sectioning and immunofluorescence staining of fundic organoids.**

Approximately 12 hrs after the addition of Dox to the medium, the fundic organoids were removed from Matrigel using ice-cold PBS and fixed with 4% paraformaldehyde in PBS at 4$^o$C for 1 hr. After washing with ice-cold PBS, the fundic organoids were resuspended in 50 μl of 5 % gelatin (Sigma-Aldrich) in PBS (37$^o$C) and incubated at 37$^o$C for 2 hrs, followed by subsequent incubation at 4$^o$C for 1 hr to allow the gelatin matrix to solidify. The resulting gelatin blocks were immersed in 10% sucrose in PBS at 4$^o$C until they sank and this procedure was repeated with 20% sucrose in PBS and then with 30% sucrose. The gelatin blocks were embedded in Optimal Cutting Temperature (OCT) compound (Tissue-Tek, Sakura Finetek, Tokyo, Japan), frozen and sectioned using a cryostat. All subsequent steps of immunofluorescence staining were performed at room temperature. The sections were permeabilized with 0.1% Triton X-100 in PBS for 30 min and washed with 0.05% Tween 20 in PBS (PBT) 4 times, followed by blocking with Block Ace (DS Pharma Biomedical, Osaka, Japan) at room temperature for 1 hr. Reactions with the appropriate primary antibodies diluted with Signal Booster (Beacle, Kyoto, Japan) were carried out at 4$^o$C overnight, followed by washing with PBT 4 times. The sections were then reacted with fluorescently labelled secondary antibodies diluted with Signal Booster at room temperature for 3 hrs and washed with PBT 4 times. Images were photographed with a laser scanning microscope Carl Zeiss LSM-710. The following antibodies were used for immunofluorescence staining: anti-E-cadherin mouse monoclonal IgG (1:500) (36/E-Cadherin; BD Biosciences), anti-Mucin 5AC mouse monoclonal IgG (1:500) (45M1; Abcam, Cambridge, UK), anti-ZO-1 mouse monoclonal IgG (1:500) (ZO1-1A12; Invitrogen), anti-GFP mouse monoclonal IgG (1:200) (1E4; MBL, Nagoya, Japan), anti-V5 tag rabbit monoclonal IgG (1:200) (D3H8Q; Cell Signaling Technology, Beverly, MA, USA), anti-T7 tag goat polyclonal IgG (1:200) (ab97964; Abcam), Alexa Fluor 488-labelled goat anti-rabbit IgG (1:1,000) (A-11034; Invitrogen), Alexa Fluor 488-labelled goat anti-mouse IgG (1:1,000) (A-11029; Invitrogen), Alexa Fluor 546-labelled goat anti-mouse IgG (1:1,000) (A-11030; Invitrogen), Alexa Fluor 594-labelled goat anti-rabbit IgG (1:1,000) (A-11037; Invitrogen), Alexa Fluor 633-labelled donkey anti-goat IgG (1:1,000) (A-21082; Invitrogen). The nuclei were stained with DAPI (Lonza, Basel, Switzerland).

**Transmission electron microscopy (TEM).**

The fundic organoids removed from Matrigel were fixed with 2.5% glutaraldehyde in 100 mM sodium cacodylate buffer at 4$^o$C for 2 hrs. After washing with the cacodylate buffer, the fundic organoids were post-fixed with 2% osmium tetroxide in the cacodylate buffer and dehydrated in a graded series of ethanol. The samples were immersed in QY-1 (n-butyl glycidyl ether) (Nisshin EM, Tokyo, Japan), embedded in Epon 812, and sectioned using an ultramicrotome. The sections were stained with uranyl acetate and lead citrate, and then examined with a transmission electron microscope HITACHI H-7650 (Hitachi, Tokyo, Japan). Morphometric analyses were performed using ImageJ software (NIH, Bethesda, MD, USA).

**Gastric biopsy specimens and ethical approval.**

To compare mucus accumulation in gastric surface mucous cells in CagA-positive *H. pylori*-infected patients with that in CagA-negative *H. pylori*-infected patients, gastric biopsy specimens obtained from Bangladesh and Thailand were selected, since the frequencies of CagA-negative *H. pylori*-infected patients found in these countries were much higher than those in East Asian countries such as Japan where almost all of *H. pylori* isolated from patients were CagA-positive[29, 30]. Biopsy materials were fixed with 10% neutral buffered formalin, embedded in a paraffin block, and sectioned for histological analysis. Gastric mucosa was stained with hematoxylin and eosin (H&E) and May-Giemsa, and degree of monocyte infiltration, neutrophil infiltration, atrophy, intestinal metaplasia and bacterial density were pathologically classified into four grades according to the updated Sydney system[31]. The sections were also subjected to the immunochemical analyses using anti-*H. pylori* rabbit polyclonal IgG (B0471; DAKO Japan, Tokyo, Japan) and anti-CagA rabbit polyclonal IgG (b-300; Santa Cruz). Genotyping of *H. pylori* isolated from biopsy specimens was performed as described[29, 30]. Briefly, the CagA genotype (EPIYA-repeat region) was determined by PCR-based direct sequencing. The study protocols above were approved by the Ethics Committee of Bangladesh Medical Research Council (Dhaka, Bangladesh), the Ethics and Research Committee of Chulalongkorn University Faculty of Medicine (Bangkok, Thailand), and the Ethics Committee of Oita University Faculty of Medicine.

**Immunofluorescence staining of gastric biopsy specimens.**

To observe mucus retention, gastric biopsy specimens which do not show marked atrophy (atrophy score 3) or intestinal metaplasia (intestinal metaplasia score equal to or greater than 1) were selected (CagA-positive *H. pylori*-infected 7, CagA-negative *H. pylori*-infected 7 from Bangladesh, CagA-positive *H. pylori*-infected 7, CagA-negative *H. pylori*-infected 5 from Thailand). The selected biopsy sections were treated for antigen retrieval in a citrate buffer (pH 6.0), permeabilized with 0.1% Triton X-100 in PBS, and blocked with Block Ace, followed by incubation with anti-Mucin 5AC mouse monoclonal IgG (1:500) (45M1; Abcam) and anti-*H. pylori* rabbit polyclonal IgG (1:200) (B0471; DAKO Japan). Alexa Fluor 488-labelled goat anti-rabbit IgG (1:1,000) (A-11034; Invitrogen) and Alexa Fluor 546-labelled goat anti-mouse IgG (1:1,000) (A-11030; Invitrogen) were used for double staining. Mucus accumulation in the surface mucous cells was classified into two categories, negative (-), 'low levels of mucus can be observed in the apical surface of the cells'; positive (+), 'high levels of mucus accumulation can be observed in the cytoplasm of the cells'. The evaluation was independently conducted by four researchers including an expert pathologist (T. U.) in a blinded manner.

## Declarations

**Data availability:**

The data that support the findings of this study are available from the corresponding author on reasonable request.

**Author Contributions:**

F. H. designed the study and wrote the manuscript, R. N., S. K., T. K., H. K., T. U., H. N., T. D. and C. L. performed experiments and analyzed data with support from A. T., T. S., S. M., N. K., K. M., T. A., M. F., Y. Y. and F. H.

**Acknowledgments:**

We thank Mses Miyuki Maki, Yuko Ono and Drs Rui-Cheng Ji and Hiroshi Tsutsumi for technical assistance, Prof Karen Guillemin, the Bloomington Drosophila Stock Center (NIH P40OD018537) and the Kyoto Stock Center for the flies, Dr Ryoko Baba and Prof Hiroyuki Morimoto for their help in generating gastric organoids, and Prof Tetsu Akiyama, Prof Yoichi Furukawa, Prof Masatsugu Moriyama, Dr Naoki Hijiya, Dr Mayumi Forster and Dr Stephen Forster for critical comments on the manuscript. This work was supported by the Japan Society for the Promotion of Science (Grant Number 15K08155) and the Discretion of the President of Oita University.

## References

1. Bray, F., Ferlay, J., Soerjomataram, I., Siegel, R. L., Torre, L. A., & Jemal, A. Global cancer statistics 2018: GLOBOCAN estimates of incidence and mortality worldwide for 36 cancers in 185 countries. *CA Cancer J Clin.* **68**, 394-424 (2018).
2. Wroblewski, L. E., Peek, R. M. Jr. & Wilson, K. T. *Helicobacter pylori* and gastric cancer: Factors that modulate disease risk. *Microbiol. Rev.* **23,** 713-739 (2010).
3. Yamaoka, Y. & Graham, D. Y. *Helicobacter pylori* and cancer pathogenesis. *Future Oncol.* **10,** 1487-1500 (2014).
4. Tegtmeyer, N., Wessler, S. & Backert, S. Role of the cag-pathogenicity island encoded type IV secretion system in *Helicobacter pylori FEBS J.* **278,** 1190-1202 (2011).
5. Hatakeyama, M. *Helicobacter pylori* CagA and gastric cancer: a paradigm for hit-and-run carcinogenesis. *Cell Host Microbe* **15,** 306-316 (2014).
6. Backert, S., Tegtmeyer, N. & Selbach, M. The versatility of *Helicobacter pylori* CagA effector protein functions: The master key hypothesis. *Helicobacter* **15,** 163-176 (2010).
7. Ekström, A. M., Held, M., Hansson, L. E., Engstrand, L., & Nyrén, O. *Helicobacter pylori* in gastric cancer established by CagA immunoblot as a marker of past infection. *Gastroenterology* **121**, 784–791 (2001).
8. Higashi, H. *et al.* SHP-2 tyrosine phosphatase as an intracellular target of *Helicobacter pylori* CagA protein. *Science* **295,** 683-686 (2002).
9. Mimuro, H., Suzuki, T., Tanaka, J., Asahi, M., Haas, R., & Sasakawa, C. Grb2 is a key mediator of *Helicobacter pylori* CagA protein activities. *Mol Cell* **10**, 745-755 (2002).
10. Suzuki, M., Mimuro, H., Suzuki, T., Park, M., Yamamoto, T., & Sasakawa, C. Interaction of CagA with Crk plays an important role in *Helicobacter pylori*-induced loss of gastric epithelial cell adhesion. *J Exp Med.* **202**, 1235-1247 (2005).
11. Saadat, I. *et al. Helicobacter pylori* CagA targets PAR1/MARK kinase to disrupt epithelial cell polarity. *Nature* **447,** 330-333 (2007).
12. Buti, L., Spooner, E., Van der Veen, A. G., Rappuoli, R., Covacci, A., & Ploegh, H. L. *Helicobacter pylori* cytotoxin-associated gene A (CagA) subverts the apoptosis-stimulating protein of p53 (ASPP2) tumor suppressor pathway of the host. *Proc Natl Acad Sci USA.* **108**, 9238-9243 (2011).
13. Amieva, M. R. *et al.* Disruption of the epithelial apical-junctional complex by *Helicobacter pylori Science* **300,** 1430-1434 (2003).
14. Crabtree, J. E., Wyatt, J. I., Trejdosiewicz, L. K., Peichl, P., Nichols, P. H., Ramsay, N., Primrose, J. N., & Lindley, I. J. Interleukin-8 expression in *Helicobacter pylori* infected, normal, and neoplastic gastroduodenal mucosa. *J Clin. Pathol.* **47**, 61-66 (1994).
15. Crabtree, J. E., Covacci, A., Farmery, S. M., Xiang, Z., Tompkins, D. S., Perry, S., Lindley, I. J., & Rappuoli, R. *Helicobacter pylori* induced interleukin-8 expression in gastric epithelial cells is associated with CagA positive phenotype. *Clin. Pathol.* **48,** 41–45 (1995).
16. Brandt, S., Kwok, T., Hartig, R., König, W., & Backert, S. NF-kB activation and potentiation of proinflammatory responses by the *Helicobacter pylori* CagA protein. *Proc Natl Acad Sci USA.* **102**, 9300-9305 (2005).
17. Uotani, T., Murakami, K., Uchida, T., Tanaka, S., Nagashima, H., Zeng, X. L., Akada, J., Estes, M. K., Graham, D. Y., & Yamaoka, Y. Changes of tight junction and interleukin-8 expression using a human gastroid monolayer model of *Helicobacter pylori Helicobacter* **24**, e12583 (2019).

18. Fukuda, M. Rab27 effectors, pleiotropic regulators in secretory pathways. *Traffic* **14,** 949-963 (2013).
19. Brand, A. & Perrimon, N. Targeted gene expression as a means of altering cell fates and generating dominant phenotypes. *Development* **118,** 401-415 (1993).
20. Botham, C. M., Wandler, A. M. & Guillemin, K. A transgenic *Drosophila* model demonstrates that the *Helicobacter pylori* CagA protein functions as a eukaryotic Gab adaptor. *PLoS Pathog.* **4,** e1000064 (2008).
21. Toba, G. *et al.* The gene search system. A method for efficient detection and rapid molecular identification of genes in *Drosophila melanogaster*. *Genetics* **151,** 725–737 (1999).
22. Pilot, F., Philippe, J. M., Lemmers, C. & Lecuit, T. Spatial control of actin organization at adherens junctions by a synaptotagmin-like protein Btsz. *Nature* **442,** 580-584 (2006).
23. Kuroda, T. S. & Fukuda, M. Rab27A-binding protein Slp2-a is required for peripheral melanosome distribution and elongated cell shape in melanocytes. *Nat Cell Biol.* **6,** 1195-1203 (2004).
24. Saegusa, C. *et al.* Decreased basal mucus secretion by Slp2-a-deficient gastric surface mucous cells. *Genes Cells* **11,** 623-631 (2006).
25. Falk, P. *et al.* An *in vitro* adherence assay reveals that *Helicobacter pylori* exhibits cell lineage-specific tropism in the human gastric epithelium. *Natl. Acad. Sci. USA* **90,** 2035–2039 (1993).
26. Furutani, M., Tsujita, K., Itoh, T., Ijuin, T. & Takenawa, T. Application of phosphoinositide-binding domains for the detection and quantification of specific phosphoinositides. *Anal Biochem.* **355,** 8-18 (2006).
27. Andrianifahanana, M., Moniaux, N. & Batra, S. K. Regulation of mucin expression: mechanistic aspects and implications for cancer and inflammatory diseases. *Biochem Biophys Acta.* **1765,** 189-222 (2006).
28. Bartfeld, S. *et al.* In vitro expansion of human gastric epithelial stem cells and their responses to bacterial infection. *Gastroenterology* **148,** 126-136 (2015).
29. Ansari, S. *et al. Helicobacter pylori* bab characterization in clinical isolates from Bhutan, Myanmar, Nepal and Bangladesh. *PLoS One* **12,** e0187225 (2017).
30. Subsomwong, P. *et al. Helicobacter pylori* virulence genes of minor ethnic groups in North Thailand. *Gut Pathog.* **9,** 56 (2017).
31. Dixon, M. F., Genta, R. M., Yardley, J. H. & Correa, P. Classification and grading of gastritis. The updated Sydney System. International Workshop on the Histopathology of Gastritis, Houston 1994. *Am J Surg Pathol.* **20,** 1161-1181 (1996).
32. Dedhia, P. H., Bertaux-Skeirik, N., Zavros, Y., & Spence, J. R. Organoid models of human gastrointestinal development and disease. *Gastroenterology* **150**, 1098-1112 (2016).
33. Kuraishy, A., Karin, M. & Grivennikov, S. I. Tumor promotion via injury- and death-induced inflammation. *Immunity* **35,** 467-477 (2011).
34. Greten, F. R. & Grivennikov, S. I. Inflammation and cancer: Triggers, mechanisms, and consequences. *Immunity* **51**, 27-41 (2019).
35. Sarkar, S., Gulati, K., Kairamkonda, M., Mishra, A., & Poluri, K. M. Elucidating protein-protein interactions through computational approaches and designing small molecule inhibitors against them for various diseases. *Curr Top Med Chem.* **18**, 1719-1736 (2018).
36. Modell, A. E., Blosser, S. L., & Arora, P. S. Systematic targeting of protein-protein interactions. *Trends Pharmacol Sci.* **37**, 702-713 (2016).
37. Thung, I., Aramin, H., Vavinskaya, V., Gupta, S., Park, J. Y., Crowe, S. E., & Valasek, M. A. Review article: the global emergence of *Helicobacter pylori* antibiotic resistance. *Aliment Pharmacol Ther* **43**, 514-533 (2016).
38. Chey, W. D., Leontiadis, G. I., Howden, C. W., & Moss, S. F. ACG clinical guideline: Treatment of *Helicobacter pylori Am J Gastroenterol.* **112**, 212-239 (2017).
39. Kuroda, T. S., Fukuda, M., Ariga, H. & Mikoshiba, K. The Slp homology domain of synaptotagmin-like proteins 1-4 and Slac2 functions as a novel Rab27A binding domain. *J Biol Chem.* **277,** 9212-9218 (2002).
40. Kuroda, T. S., Fukuda, M., Ariga, H. & Mikoshiba, K. Synaptotagmin-like protein 5: a novel Rab27A effector with C-terminal tandem C2 domains. *Biochem Biophys Res Commun.* **293,** 899-906 (2002).
41. Yusa, K., Rad, R., Takeda, J. & Bradley, A. Generation of transgene-free induced pluripotent mouse stem cells by the piggyBac transposon. *Methods* **6,** 363-369 (2009).
42. Ding, S. et al. Efficient transposition of the piggyBac (PB) transposon in mammalian cells and mice. *Cell* **122,** 473-483 (2005).
43. Takahashi, M. et al. Downregulation of WDR20 due to loss of 14q is involved in the malignant transformation of clear cell renal cell carcinoma. *Cancer Sci.* **107,** 417-423 (2016).
44. Yusa, K., Zhou, L., Li, M. A., Bradley, A. & Craig, N. L. A hyperactive piggyBac transposase for mammalian applications. *Proc Natl Acad Sci USA.* **108,** 1531-1536 (2011).
45. Miyoshi, H., Ajima, R., Luo, C. T., Yamaguchi, T. P. & Stappenbeck, T. S. Wnt5a potentiates TGF-β signaling to promote colonic crypt regeneration after tissue injury. *Science* **338,** 108-113 (2012).

## Figures

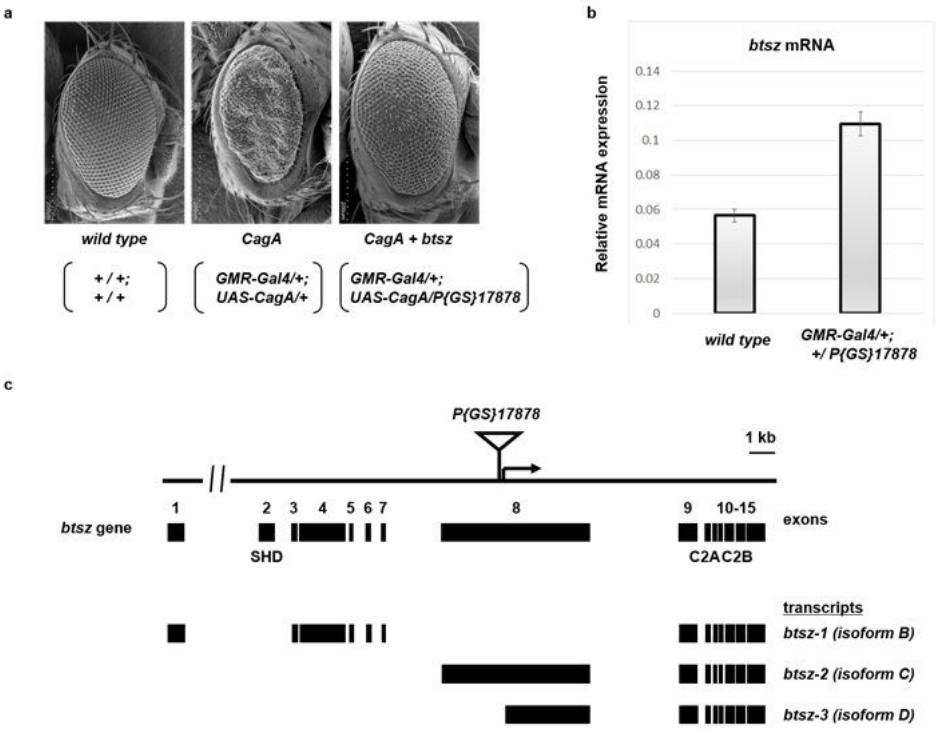


## Figure 1

Forced expression of btsz suppresses CagA-induced rough eye phenotype in Drosophila. a, Electron micrographs of eyes in flies of wild type control (+/+; +/+), expressing CagA alone (GMR-Gal4/+; UAS-CagA/+), and coexpressing CagA and btsz (GMR-Gal4/+; UAS-CagA /P{GS}17878). b, btsz mRNA expression in eyes of wild type control (+/+; +/+) and the GMR-Gal4/+; P{GS}17878/+ line. The relative mRNA expression levels are normalized to rpL32 as an internal control. Each bar represents the mean ± SD of three samples. c, Schematic diagram of the btsz locus, its transcripts, and the P{GS}17878 insertion site. The exons are shown as filled boxes and their encoding protein domains, SHD and C2AC2B, are indicated. Direction of the P{GS} vector-flanking gene transcription under the control of GAL4 is shown by an arrow.

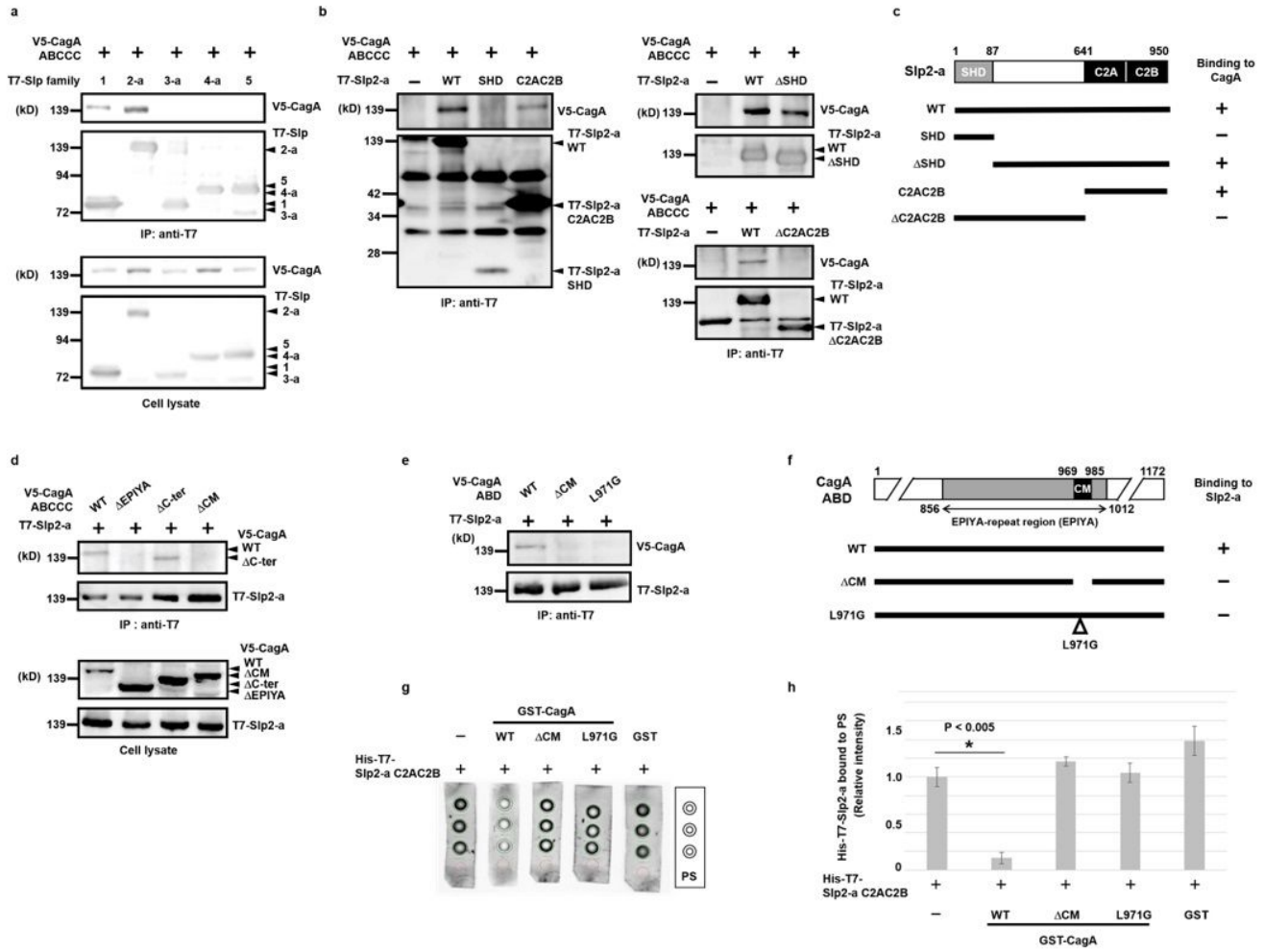


## Figure 2

CagA interacts with Slp2-a and inhibits its binding to membrane phospholipids. a, Co-immunoprecipitation of CagA with Slp2-a. V5-CagA and T7-Slp1-5 were co-expressed in COS-7 cells. T7-Slp1-5 were immunoprecipitated (IP) with anti-T7 antibodies and associated V5-CagA ABCCC was detected by immunoblotting (IB) with anti-V5 antibodies. b, CagA binds to Slp2-a C2AC2B. c, A schematic diagram of the Slp2-a deletion mutants used in co-immunoprecipitation with CagA and the results of binding. d, Slp2-a binds to CM of CagA ABCCC. e, Slp2-a binds to CM of CagA ABD. f, A schematic diagram of the CagA ABD deletion and substitution mutants and the results of binding to Slp2-a. g, CagA inhibits interaction between PS and Slp2-a C2AC2B. PS-spotted nitrocellulose membranes were incubated with His-T7-Slp2-a C2AC2B in the presence of GST, GST-CagA WT, GST-CagA CM or GST-CagA L971G. His-T7-Slp2-a C2AC2B bound to PS was detected with anti-T7. h, Densitometric analysis of His-T7-Slp2-a C2AC2B binding to PS (n = 3). Results are shown as the mean ± SD. P < 0.005 by Student's t test.

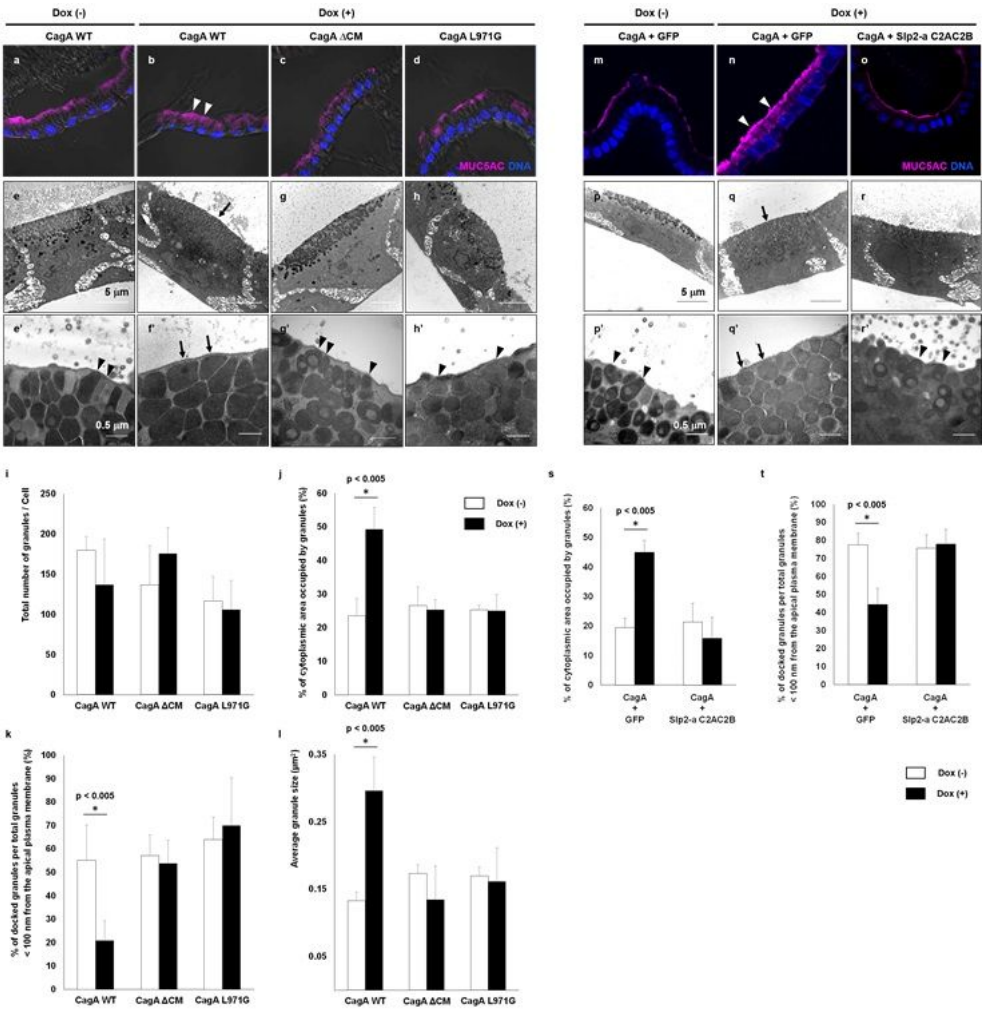


## Figure 3

CagA inhibits Slp2-a-mediated docking of mucous granules to the apical plasma membrane and disrupts exocytosis in the gastric surface mucous cells. Expression of CagA WT, CM, or L971G, and co-expression of CagA WT with GFP as a control or with Slp2-a C2AC2B were induced with doxycycline, Dox (+). Immunofluorescence shows magenta staining for MUC5AC and blue staining for nuclei. a-d, Excessive mucus accumulation beneath the apical plasma membrane in the CagA WT-expressing cells (arrowheads in b). e-h, Marked accumulation of mucous granules beneath the apical plasma membrane in the CagA WT-expressing cells (arrow in f). e'-h', Inhibition of docking of mucous granules to the apical plasma membrane in the CagA WT-expressing cells (arrows in f'). Arrowheads in (e', g', h') indicate docked granules. i-l, Morphometric analyses of CagA WT, CM, and L971G-expressing cells. Error bars indicate standard deviations. P < 0.005 by Student's t test. i, Total number of granules / cell (n = 5). j, % of cytoplasmic area occupied by granules (n = 5). k, % of docked granules per total granules < 100 nm from apical plasma membrane (n > 188 granules). l, Average granule size (m2) (n > 560 granules). m-r, Exogenously expressed Slp2-a C2AC2B, but not GFP, reduces the mucus retention and inhibition of docking of mucous granules to the membrane caused by CagA WT. Excessive mucus accumulation (arrowheads in n), highly accumulated mucous granules (arrow in q) and inhibition of granule docking (arrows in q') in the cells co-expressing CagA WT and GFP. Arrowheads in (p', r') indicate docked granules. s, t, Morphometric analyses of CagA WT + GFP and + Slp2-a C2AC2B-expressing cells. s, % of cytoplasmic area occupied by granules (n = 5). t, % of docked granules per total granules < 100 nm from apical plasma membrane (n > 100 granules).

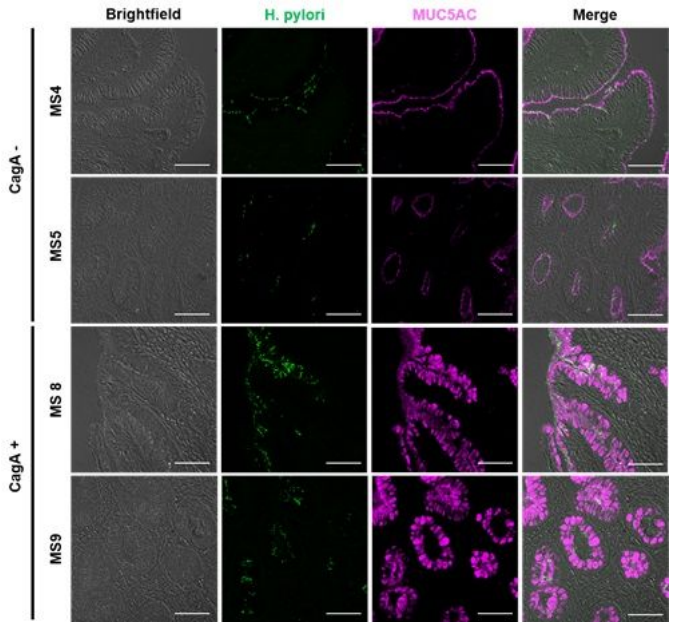


**Figure 4**

Excessive mucus accumulation in the gastric surface mucous cells of CagA-positive H. pylori-infected patients. Representative immunofluorescence images of gastric biopsy specimens of H. pylori-infected patients with gastritis shows magenta staining for MUC5AC and green staining for H. pylori. The CagA status was determined by immunohistochemistry using anti-CagA and genome sequencing. The patient's number is indicated. Scale bars, 50 m.

## Supplementary Files

This is a list of supplementary files associated with this preprint. Click to download.

- Ninomiyaetal010321SupplementaryInformation.docx